KSME International Journal, Vol. 16, No. 5, pp. 639~646, 2002

Steady State and Transient Characteristics of a Rubber Belt CVT with Mechanical Actuatiors

Hyunsuk Kim
Hyundai Motor Company,
772-1, Changduk-dong, Whasung-shi, Kyunggi-do, 445-706, Korea
Heera Lee
Graduate Student, School of Mechanical Engineering, Sungkyunkwan University,
300 Chunchun-dong, Suwon, Kyunggi-do, 440-746, Korea
Hanlim Song
Department of Computer Aided Mechanical Design, Ansan College of Technlolgy,
170, Choji-dong, Ansan, Kyunggi-do, 425-792, Korea
Hyunsoo Kim*
Professor, School of Mechanical Engineering, Sungkyunkwan University,
300 Chunchun-dong, Suwon, Kyunggi-do, 440-746, Korea

In this paper, thrust equations for a rubber belt CVT are derived by considering the geometry and mechanism of the mechanical actuators. In order to solve the thrust equations, an algorithm to calculate the speed ratio is suggested for the given driver speed and load torque based on the actuator characteristic equations and existing formula for the belt thrust forces. Experiments are performed to investigate the driver speed-load torque-speed ratio characteristics at a steady state. The speed and torque efficiencies are measured and used to modify the actuator equations. It is found that the modified equations well predict the steady state characteristics. In addition, the shift dynamic model for a rubber belt CVT is derived experimentally. Simulation results of the CVT shift dynamics are in good accordance with the experiments and it is noted that different coefficients are required to describe the CVT shift dynamics for the upshift and the downshift.

Key Words : Rubber Belt, CVT, Actuator, Shift Dynamics

1. Introduction

It is well known that CVT is able to move the engine operation point independent of the vehicle speed, which provides improvement of fuel economy by 10~15% compared with that of 4-speed automatic transmission. A rubber belt CVT has been used in small power vehicles such as scooters, and leisure vehicles due to its limited torque capacity. Recently, a dry CVT made of rubber and aluminum alloy has been used in 800cc class passenger car and it is expected that applications of rubber based CVTs will be increased. In the rubber belt CVT drive, power can be transmitted under relatively low thrust owing to the rubber's high coefficient of friction, which enables power transmission by pure mechanical actuators such as centrifugal rollers and torque cams which do not need external power. Centrifugal rollers and torque cams have been widely used in the rubber belt CVT as the mechanical actuators and performance of the CVT depends directly on the characteristics of

* Corresponding Author,
E-mail : hskim@me.skku.ac.kr
TEL : +82-31-290-7438; **FAX** : +82-31-290-7473
Professor, School of Mechanical Engineering, Sungkyunkwan University, 300 Chunchun-dong, Suwon, Kyunggi-do 440-746, Korea. (Manuscript **Received** September 6, 2001; **Revised** January 31, 2002)

these actuators. Therefore, in order to estimate the performance of the rubber belt CVT drive with mechanical actuators, it is required to take into account the actuator characteristics as well as the belt transmission characteristics.

The mechanisms of the centrifugal roller and torque cam were analyzed (Oliver, 1973) without consideration of CVT belt transmission characteristics. As for the rubber V-belt mechanisms, extensive analyses were performed related with sliding theory, slip, torque, power loss and etc. (Gerbert, 1999). From the practical design point of view, Worley's formula for the driver pulley thrust (Worley, 1985) and Miloiu's formula for the driven thrust (Miloiu, 1969) have been widely used due to its simplicity.

Most equations of the belt and the actuator mechanisms derived so far have structures to calculate the thrust when the speed ratio is given as an input. From the design point of view, however, it is useful to obtain the speed ratio when the driver and driven thrusts are given as inputs. Furthermore, most such work has considered the actuators separately from the belt or vice versa. Few studies have been reported on the rubber belt CVT as a total system including the belt and the actuators.

In this paper, an algorithm to obtain the speed ratio for the given driver speed and load torque is presented for the rubber belt CVT based on the actuator equations and an existing formula for the speed ratio-torque-thrust relationship. Using the algorithm, steady-state characteristics for a CVT system with mechanical actuators are investigated by simulations and experiments. In addition, shift dynamics for the rubber belt CVT is obtained and used to predict transient responses of the CVT system.

2. Mechanism of Rubber Belt CVT System

2.1 Belt transmission

A speed ratio-torque-thrust relationship of the rubber belt CVT is represented as,

$$F_R=\frac{T_1}{2}\theta_R\left[\frac{1-\mu\tan\frac{\alpha}{2}}{\mu+\tan\frac{\alpha}{2}}\right] \tag{1}$$

$$F_N=\frac{T_2}{2}(\theta_N-\theta_{Na})\left[\frac{1-\mu\tan\left(\frac{\alpha}{2}\right)}{\mu+\tan\left(\frac{\alpha}{2}\right)}\right]+\frac{T_1-T_2}{2\mu}\cos\frac{\alpha}{2} \tag{2}$$

where F is the thrust, θ is the arc of contact, μ is the coefficient of friction, α is the V-wedge angle, and T_1, T_2 are the tight side and the slack side belt tension, respectively. The subscript R and N denote "driver" and "driven," respectively.

2.2 Centrifugal roller

The centrifugal roller is used as a driver pulley actuator. The centrifugal roller generates an axial thrust force depending on the rotational speed. In Fig. 1, a schematic diagram of the centrifugal roller is shown. From Fig. 1, the thrust by the centrifugal roller F_R is obtained as,

$$F_R=Z\times F_{cl}(\sin\beta-\mu_c\cos\beta) \tag{3}$$

where Z is the number of rollers, and F_{cl} is the normal force applied to the movable flange by the roller expressed by

$$F_{cl}=F_{cen}\times\left[\frac{\sin\gamma-\mu_c\cos\gamma}{(\sin\gamma-\mu_c\cos\gamma)(\cos\beta+\mu_c\sin\beta)+(\sin\beta-\mu_c\cos\beta)(\cos\gamma+\mu_c\sin\gamma)}\right] \tag{4}$$

where F_{cen} is the centrifugal force and μ_c is the coefficient of friction between the roller and the flange. β and γ are the geometrical angles as shown in Fig. 1. The radius is determined from the geometry depending on the speed ratio.

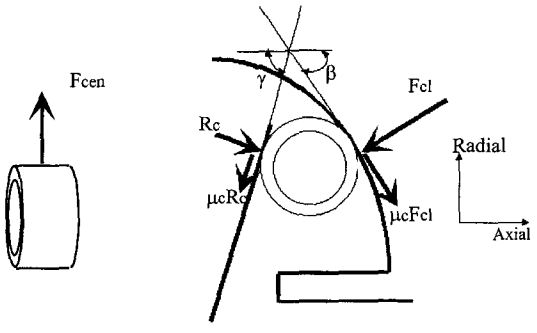

Fig. 1 Free body diagram of centrifugal roller

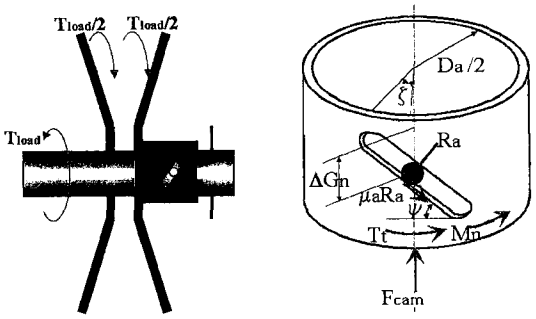

Fig. 2 Torque cam

2.3 Torque cam

The driven pulley thrust is required to provide the belt clamping force to transmit a torque between the belt and the pulley. In the rubber belt CVT, a torque cam is widely used as the driven pulley actuator(Fig. 2). The torque cam provides the thrust force depending on the magnitude of the applied load torque. When the load torque T_{load} increases, the movable flange moves to the belt side. Correspondingly, the belt pitch radius increases, which results in the downshift. The driven pulley thrust applied to the belt can be represented as a sum of the spring force F_S and the torque cam force F_{cam} as,

$$F_N = F_S + F_{cam} \tag{5}$$

F_{cam} is obtained from the force equilibrium in the axial direction from Fig. 2

$$F_{cam} = \frac{2}{D_a}\left[\frac{D_N}{4}(T_1 - T_2) + M_{n0} + k_t\xi\right]\frac{(\cos\varphi + \mu_a \sin\varphi)}{(\sin\varphi - \mu_a \cos\varphi)} \tag{6}$$

where D_a is the torque cam diameter, D_N is the belt pitch diameter, φ is the torque cam angle, μ_a is the friction coefficient, k_t is the spring constant, ξ is the rotational displacement of the spring which changes depending on the movable flange displacement (i.e., the speed ratio).

3. Steady State Characteristics

For the rubber belt CVT with mechanical actuators, the speed ratio i is determined when the primary speed and the load torque are given. In order to solve the thrust equations of the belt and the actuators, Eqs. (1)~(6), design parameters such as the arc of contact, a belt pitch diameter, and a roller angle are required to calculate the thrust. However, these parameters can be determined only when the speed ratio is given. In addition, from the viewpoint of the practical design, it is convenient to predict the speed ratio when the driver speed and the load torque are given. Therefore, in this study, an algorithm to calculate a speed ratio for given driver speed and load torque is suggested as shown in Fig. 3.

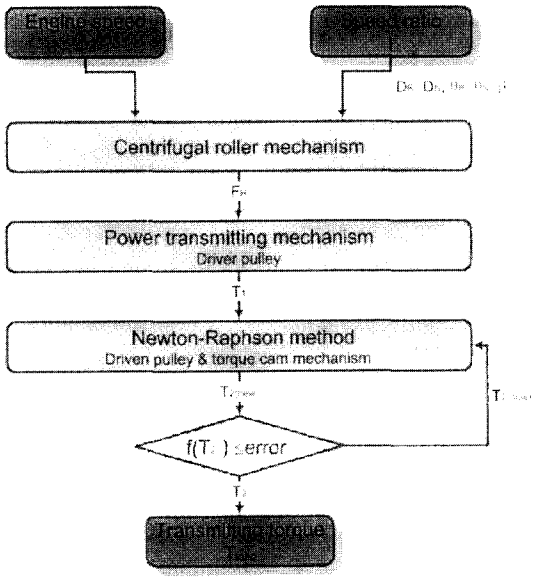

Fig. 3 Flow chart

Calculation procedure is as follow : firstly, the driver thrust is calculated from the centrifugal roller mechanism for the given inputs such as the driver speed, ω_P, the driver and the driven belt pitch diameters, D_R and D_N, the arcs of contact, θ_R and θ_N, and the roller angle β. Since D_R, D_N, θ_R, θ_N and β need to be determined from the speed ratio i, an arbitrary speed ratio is assumed for the calculation. Using the driver thrust and the belt mechanism, Eq. (1), the tight side belt tension, T_1 is obtained. Next, the slack side belt tension T_2 is determined from Egs. (2) and (6) for the belt and the torque cam by the Newton-Rapson method. This procedure is repeated until the numerical error converges within the error bound. The load torque can be obtained from T_1, T_2 and the belt radius. This algorithm give a 3-D map for the driver speed-torque-speed ratio.

4. Experiment

Figure 4 shows a CVT tester which is designed for the experiment. Power is transmitted from the DC motor① to CVT③ via the driver shaft② and is absorbed in the dynamometer⑤. Input torque and load torque are measured by the torque sensor⑥ and dynamometer⑤. The driver and driven speeds are also measured by the speed sensor and the dynamometer respectively. The belt pitch radius is measured by a laser displac -ment sensor at the driver and driven pulleys. The driven pulley and the dynamometer are assembled on the moving plate⑦ mounted on the linear motion guide⑩. The belt tension is measured by load cell⑧.

In Fig. 5, the experimental results for the driver speed-torque-speed ratio are compared with the simulation results at a steady state. It is noted from Fig. 5 that the load torques by the experiment are lower than the simulation results for $i=1.5$ and $i=2.0$. Since the simulations were carried out by assuming that power transmission efficiency $\eta_p=100\%$, effects of the torque and the speed efficiency on the CVT system need to be considered.

Figure 6 shows the CVT efficiency measured from the experiments. In the experiments, the power and speed efficiencies are measured and are plotted with respect to the traction coefficient λ. λ is defined as,

$$\lambda=\frac{T_1-T_2}{T_1+T_2} \tag{7}$$

The speed efficiency is obtained by measuring the driver and driven speeds, and the driver and driven belt pitch radii. As shown in Fig. 6, it is considered that the speed efficiency is almost constant as $\eta_\omega=95\%$. However, the torque and power efficiencies increase as the traction coefficient λ increases up to $\lambda=0.14$ and remain almost constant. Therefore, the belt and actuator equations Eq. (1)-Eq. (6) derived previously should be modified by considering the speed and torque efficiencies. The modification procedure is as follows :

- modify the geometric parameters such as a belt pitch radius and a roller contact angle using the speed ratio i multiplied by the speed efficiency η_ω.
- modify the actual load torque by multiplying the torque efficiency η_t as

$$T_{actual}=\eta_t T_n \tag{8}$$

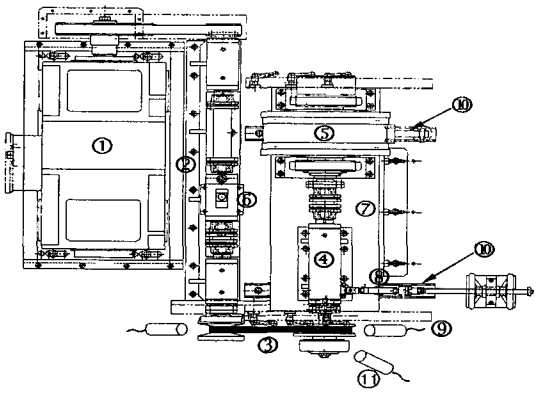

Fig. 4 Schematic diagram of CVT tester

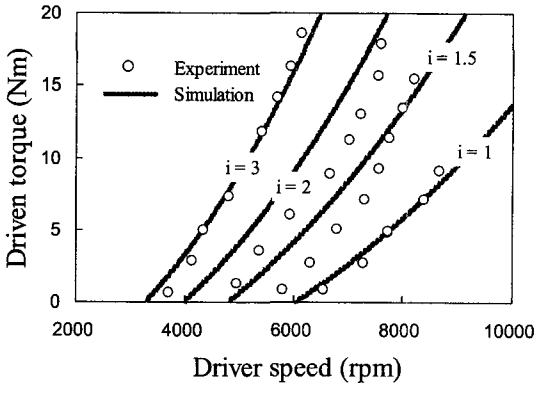

Fig. 5 Comparison of steady state characteristics

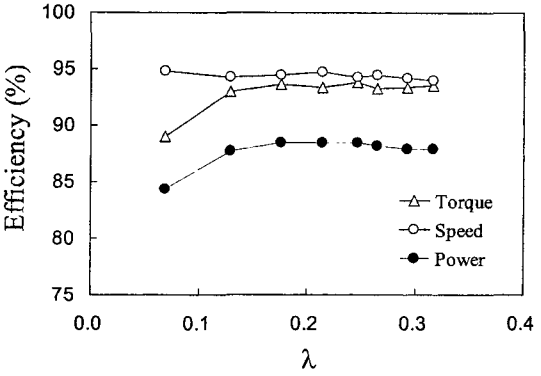

Fig. 6 Efficency

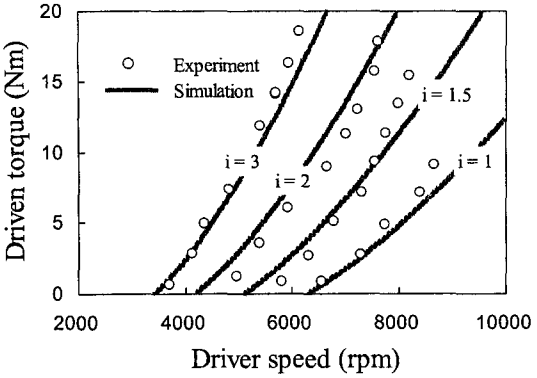

Fig. 7 Comparison of experimental results with simulation by considering efficiency

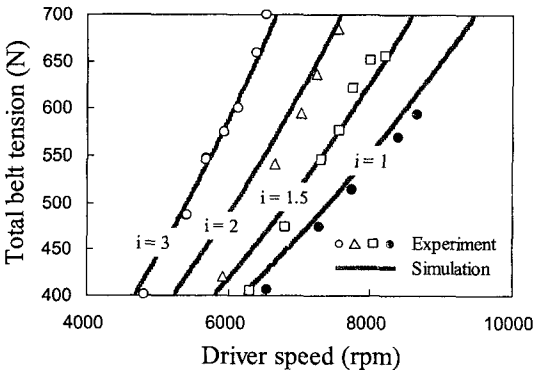

Fig. 8 Total belt tension

Figure 7 shows comparison of the experimental results with the simulation using the modified equations by considering the efficiencies. It is seen from Fig. 7 that the experimental results fit the simulation results better than those in Fig. 5. In Fig. 8, the experimental results of the total belt tension are compared with the simulation results. It is seen from Fig. 8 that the simulation results agree with the experiments in overall trend.

Figure 9 shows a variogram at a steady state. The variogram is constructed to simulate the performance of a scooter which consists of a rubber belt CVT with mechanical actuators and a 125cc engine. In the experiment, the driven speed is measured for a given driver speed and a driver torque. The driver torque is chosen to simulate the engine characteristics at a wide open throttle. As shown in Fig. 9 (a) and (b), the upshift is obtained as the driver speed increases while the

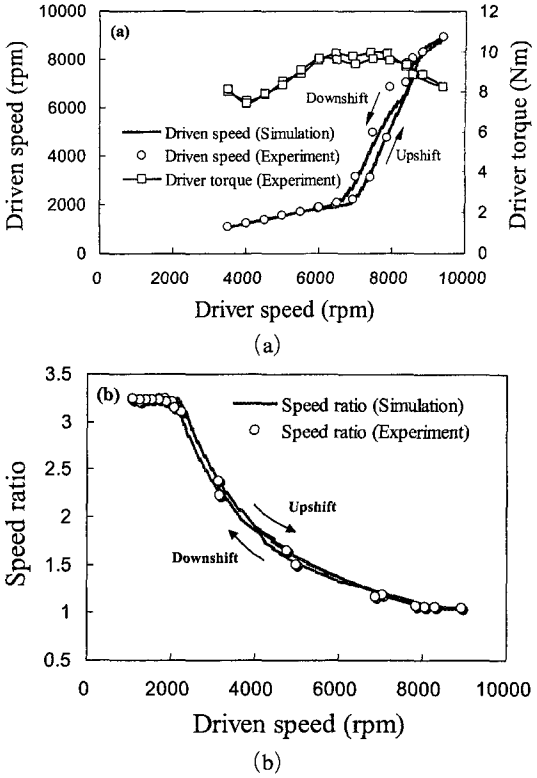

Fig. 9 Variogram (a) and speed ratio (b)

downshift is achieved as the driver speed decreases. As shown in Fig. 9, the simulation results agree with the experiments.

From Fig. 7-Fig. 9, it is found that the algorithm suggested in this study can be used to predict the steady state characteristics of the rubber belt CVT with mechanical actuators.

5. Transient Characteristics

In order to investigate the transient characteristics of the rubber belt CVT, it is essential to understand the CVT shift dynamics. As for the rubber belt CVT, few literature has been reported on the shift dynamics. In this study, the rubber belt CVT shift dynamics is obtained.

At a steady state, the rubber belt transmission can be described by the steady state equations, Eq. (1)-Eq. (2), which are derived from the radial and tangential force equilibrium of the belt. However, during the transient state when the belt pitch radius changes, kinetic friction occurs in the

radial direction while other forces are acting in the same manner with the forces at a steady state. Since inertia force of the belt is relatively small compared to the other forces, it is expected that the shift dynamics is governed by the kinetic friction force which depends on the relative velocity of the belt radial motion. In this study therefore, the following first order system is proposed as the rubber belt CVT shift dynamics.

$$\frac{di}{dt}=\alpha(i)\,\omega_R(F_R-F_R^*) \tag{9}$$

where $\alpha(i)$ is the coefficient which is a function of the speed ratio, ω_R is the driver speed, F_R is the driver thrust, and F_R^* is the driver thrust at a steady state for the given speed ratio and the torque. The same type of Eq. (9) was suggested for a metal belt CVT based on the experiments (Ide, Uchiyama and Kataoka, 1996). In order to derive Eq. (9), the coefficient $\alpha(i)$ needs to be determined. In Eq. (9), F_R^* can be calculated for the given speed ratio and torque from Eq. (1).

Experiments are carried out to obtain $\alpha(i)$. Figure 10 shows the response of the CVT ratio for the driver speed.

The experimental results of the CVT ratio and the input driver speed are plotted with thin curve. The upshift(a) is performed by increasing the driver thrust. Since the driver thrust depends on the driver speed, the upshift is obtained by increasing the driver speed. In the experiment, the upshift is obtained by increasing the primary speed from 4000rpm to 8000rpm while the load torque is maintained as T_n=10Nm. The downshift(b) is performed by decreasing the speed from 8000rpm to 4000rpm speed.

Figure 11 shows the experimental results of the CVT ratio response for various load torques. In the experiments, the load torque is varied between 0Nm to 15Nm while the driver speed is maintained as ω_R=5000rpm. As expected from

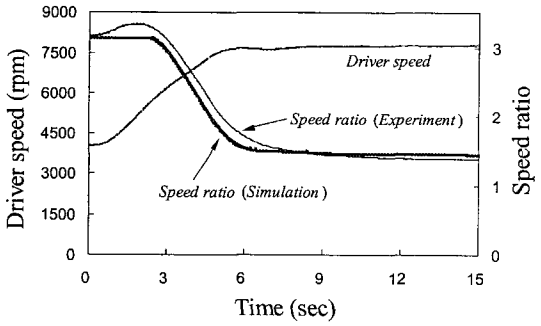

(a) Increasing driver speed
(ω_p=4000rpm → 8000rpm, T_n=10Nm)

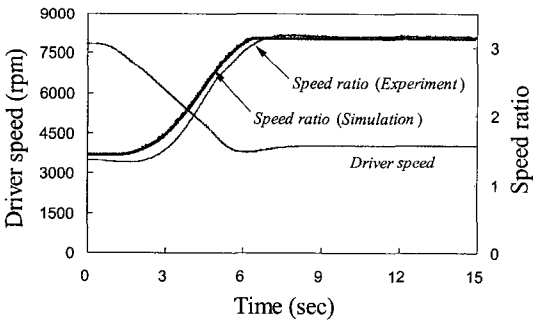

(b) Decreasing driver speed
(ω_p=8000rpm → 4000rpm, T_n=0Nm)

Fig. 10 Transient response of CVT ratio for driver speed

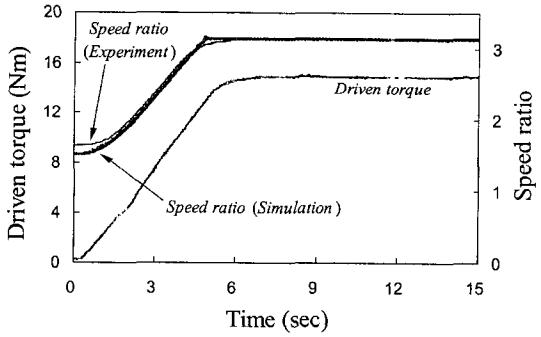

(a) Increasing driven torque
(ω_p=5000rpm, T_n=0Nm → 15Nm)

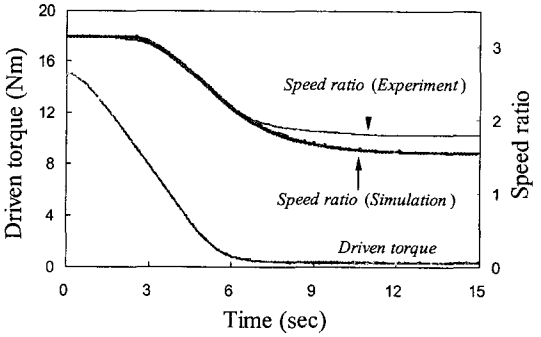

(b) Decreasing driven torque
(ω_p=5000rpm, T_n=15Nm → 0Nm)

Fig. 11 Transient response of speed ratio for load torque

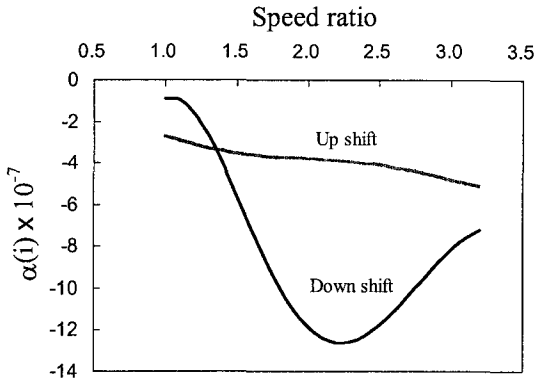

Fig. 12 $\alpha(i)$

the steady state relationship in Fig. 7, the CVT ratio downshifts for the increasing load torque (a) and upshift for the decreasing load torque(b).

Similar experiments are carried out for various speeds and load torques. Using Eq. (9) and the experimental results, $\alpha(i)$ is obtained by a trial and error manner, which best fits best to the experimental results, and is shown on Fig. 12.

As shown on Fig. 12, a different $\alpha(i)$ is obtained for the upshift and downshift, which is an unique characteristic compared to the metal belt CVT, whose dynamics is represented only by a single $\alpha(i)$ for both the upshift and downshift. The reason why different $\alpha(i)$ is required for the upshift and downshift is explained as follows : It is well known that self locking occurs in the driver pulley at a steady state for a rubber V-belt drive, which means that the belt pitch radius is almost constant along the arc of contact and a static friction occurs in the radialy outward direction on the belt. When the driver belt pitch radius decreases in the downshift, the friction force on the belt occurs in the radialy outward direction, which is the same direction with the friction in a steady state. Therefore, it can be assumed that the similar force equilibrium with a steady state is applied and the belt pitch radius remains constant along the arc of contact at each moment of the shifting due to the pseudo-self locking in the transient state. For the upshift, the driver belt pitch radius increases and correspondingly, the friction acts in the radialy inward direction, which is opposite to the friction state at a steady state. The pseudo-self locking cannot happen during the upshift since the friction on the belt acts in the radialy inward direction. Therefore, the belt pitch radius does not remain constant along the arc of contact, which means that kinetic friction occurs in the circumferential direction as well as the radial direction. This causes a different shift dynamics from the downshift and it is considered that this phenomenon requires a different $\alpha(i)$ to describe the rubber belt CVT shift dynamics for the upshift and downshift.

In Fig. 10-Fig. 11, simulation results (thick curve) of the CVT shift dynamics are compared with the experimental results. The simulations are performed using Eq. (9) and $\alpha(i)$ in Fig. 12. It is seen from Fig. 10-Fig. 11 that the rubber belt CVT shift model suggested in this study is able to predict the real shift dynamics reasonably well. The overshoot in the initial stage of the upshift which is seen in the experimental curve is due to the inertial effect of the rotating parts in the motor, pulley and dynamometer.

6. Conclusion

Thrust equations for a rubber belt CVT are derived by considering the actuator characteristics. In order to solve the thrust equations, an algorithm to calculate the speed ratio is suggested for the given driver speed and load torque based on the actuator equations and the existing formula for the belt thrust forces. Experiments are performed to investigate the driver speed-load torque-speed ratio characteristics at a steady state. From the experiments, the speed and torque efficiencies are measured and are used to modify the belt and actuator equations. It is found that the modified equations well predict the steady state characteristics. In addition, a rubber belt CVT shift dynamic model is derived. Simulation results of the CVT shift dynamics are in good accordance with the experiments and it is noted that different coefficients are required to describe the CVT shift dynamics for the upshift and downshift.

References

Dolan, J. P. and Worley, W. S., 1985, "Closed-form Approximations to the Solution of V-Belt Force and Slip Equations," *Trans. ASME, J. of Mechanical Design*, Vol. 107, pp. 292~300.

Gerbert, G., 1999, "Traction Belt Mechanics," *Chalmers University of Technology*.

Ide, T., Uchiyama, H. and Kataoka, R., 1996, "Experimental Investigation on Shift Speed Characteristics of a Metal V-Belt CVT," *Proc. Of Int. Conf. On CVT*, pp. 59~64.

Miloiu, G., 1969, "Druckkraft in Stufenlosen Getrieben II," *Antriebstechnik*, Vol. 8, pp. 450~459.

Oliver, L. R., Hornung, K. G., Swenson, J. E. and Shapiro, H. N., 1973, "Design Equations for a Speed and Torque Controlled Variable Ratio V-Belt Transmission," *SAE Paper #730003*.